

# Interleukin 11 therapy causes acute heart failure and its use in patients should be reconsidered

Mark Sweeney MB BChir<sup>1,2,3</sup>, Katie O’Fee MRes<sup>1,2</sup>, Chelsie Villanueva-Hayes MSc<sup>1,2</sup>, Ekhlas Rahman MSc<sup>1,2</sup>, Michael Lee PhD<sup>4</sup>, Henrike Maatz PhD<sup>5,6</sup>, Eric L. Lindberg PhD<sup>5</sup>, Konstantinos Vanezis PhD<sup>1,2,4</sup>, Ivan Andrew BSc<sup>1,2</sup>, Emma R. Jennings<sup>2</sup>, Wei-Wen Lim PhD<sup>7,8</sup>, Anissa A Widjaja PhD<sup>8</sup>, Norbert Hubner MD<sup>5,6,9</sup>, Paul J.R. Barton PhD<sup>1,2,4,10</sup>, Stuart A Cook PhD<sup>1,2,7,8</sup>

<sup>1</sup>MRC-London Institute of Medical Sciences, Hammersmith Hospital Campus, London, UK.

<sup>2</sup>Institute of Clinical Sciences, Faculty of Medicine, Imperial College, London, UK.

<sup>3</sup>Wellcome Trust / NIHR 4i Clinical Research Fellow, Imperial College, London, UK.

<sup>4</sup>National Heart and Lung Institute, Imperial College, London, UK.

<sup>5</sup>Cardiovascular and Metabolic Sciences, Max Delbrück Center for Molecular Medicine in the Helmholtz Association (MDC), Berlin, Germany.

<sup>6</sup>DZHK (German Centre for Cardiovascular Research), Partner Site Berlin, Berlin, Germany.

<sup>7</sup>National Heart Research Institute Singapore, National Heart Centre Singapore, Singapore.

<sup>8</sup>Cardiovascular and Metabolic Disorders Program, Duke-National University of Singapore Medical School, Singapore.

<sup>9</sup>Charite, Universitätsmedizin Berlin, Berlin, Germany.

<sup>10</sup>Royal Brompton and Harefield Hospitals, Guy’s and St. Thomas’ NHS Foundation Trust, London UK

## Short title:

Acute cardiac toxicities of interleukin 11

## Address for correspondence:

Dr Mark Sweeney, London Institute of Medical Science, Imperial College London. W12 0NN. [msweeney@ic.ac.uk](mailto:msweeney@ic.ac.uk) or Professor Stuart Cook, London Institute of Medical Science, Imperial College London, W12 0NN. [stuart.cook@imperial.ac.uk](mailto:stuart.cook@imperial.ac.uk)

**Total word count:** 8,610

**Manuscript main text word count:** 4,544

## Abstract

### Background

Interleukin 11 (IL11) was initially thought important for platelet production, which led to recombinant IL11 being developed as a drug to treat thrombocytopenia. IL11 was later found to be redundant for haematopoiesis and its use in patients is associated with unexplained cardiac side effects. Here we identify previously unappreciated and direct cardiomyocyte toxicities associated with IL11 therapy.

### Methods

We injected recombinant mouse IL11 (rmIL11) into mice and studied its molecular effects in the heart using immunoblotting, qRT-PCR, bulk RNA-seq, single nuclei RNA-seq (snRNA-seq) and ATAC-seq. The physiological impact of IL11 was assessed by echocardiography *in vivo* and using cardiomyocyte contractility assays *in vitro*. To determine the activity of IL11 specifically in cardiomyocytes we made two cardiomyocyte-specific *Il11ra1* knockout mouse models using either AAV9-mediated and *Tnnt2*-restricted (vCMKO) or *Myh6* (m6CMKO) Cre expression and an *Il11ra1* floxed mouse strain. In pharmacologic studies, we studied the effects of JAK/STAT inhibition on rmIL11-induced cardiac toxicities.

### Results

Injection of rmIL11 caused acute and dose-dependent impairment of left ventricular ejection fraction (saline (2  $\mu$ L/kg), 60.4% $\pm$ 3.1; rmIL11 (200 mcg/kg), 31.6% $\pm$ 2.0;  $p$ <0.0001,  $n$ =5). Following rmIL11 injection, myocardial STAT3 and JNK phosphorylation were increased and bulk RNA-seq revealed upregulation of pro-inflammatory pathways (TNF $\alpha$ , NF $\kappa$ B and JAK/STAT) and perturbed calcium handling. SnRNA-seq showed rmIL11-induced expression of stress factors (*Ankrd1*, *Ankrd23*, *Xirp2*), activator protein-1 (AP-1) transcription factor genes and *Nppb* in the cardiomyocyte compartment. Following rmIL11 injection, ATAC-seq

identified epigenetic enrichment of the *Ankrd1* and *Nppb* genes and stress-responsive, AP-1 transcription factor binding sites. Cardiomyocyte-specific effects were examined in vCMKO and m6CMKO mice, which were both protected from rmIL11-induced left ventricular impairment and molecular pathobiologies. In mechanistic studies, inhibition of JAK/STAT signalling with either ruxolitinib or tofacitinib prevented rmIL11-induced cardiac dysfunction.

## Conclusions

Injection of IL11 directly activates JAK/STAT3 in cardiomyocytes to cause acute heart failure. Our data overturn the earlier assumption that IL11 is cardioprotective and explain the serious cardiac side effects associated with IL11 therapy, which questions its continued use in patients.

## 62 Clinical Perspective

### 63 What is new?

- 64 • Injection of IL11 to mice causes acute and dose-dependent left ventricular impairment
- 65 • IL11 activates JAK/STAT3 in cardiomyocytes to cause cell stress, inflammation and
- 66 impaired calcium handling
- 67 • These data identify, for the first time, that IL11 is directly toxic in cardiomyocytes,
- 68 overturning the earlier literature that suggested the opposite

### 69 What are the clinical implications?

- 70 • Recombinant human IL11 (rhIL11) is used as a drug to increase platelets in patients
- 71 with thrombocytopenia but this has severe and unexplained cardiac side effects
- 72 • We show that IL11 injection causes cardiomyocyte dysfunction and heart failure, which
- 73 explains its cardiac toxicities that were previously thought non-specific
- 74 • These findings have immediate translational implications as they question the
- 75 continued use of rhIL11 in patients around the world

76

## 77 Abbreviations

<b>AAV9</b>	Adeno-associated virus serotype 9
<b>ANOVA</b>	Analysis of variance
<b>AP-1</b>	Activator protein 1
<b>ATACseq</b>	Assay for transposase-accessible chromatin with sequencing
<b>Bpm</b>	Beats per minute
<b>CM</b>	Cardiomyocyte
<b>ECG</b>	Electrocardiogram
<b>EGFP</b>	Enhanced green fluorescent protein
<b>ERK</b>	Extracellular signal regulated kinase
<b>FDR</b>	False discovery rate
<b>FOSL2</b>	FOS like 2
<b>GAPDH</b>	Glyceraldehyde-3-phosphate dehydrogenase
<b>GCS</b>	Global circumferential strain
<b>GSEA</b>	Gene set enrichment analysis
<b>HR</b>	heart rate
<b>IL6</b>	Interleukin 6
<b>IL11</b>	Interleukin 11
<b>IL11RA1</b>	Interleukin 11 receptor A1
<b>IP</b>	Intraperitoneal
<b>JAK</b>	Janus kinase
<b>JNK</b>	c-Jun N-terminal kinase
<b>KEGG</b>	Kyoto encyclopaedia of genes and genomes
<b>LV</b>	Left ventricle
<b>LVEF</b>	Left ventricular ejection fraction
<b>PBS</b>	Phosphate buffered saline
<b>PCR</b>	Polymerase chain reaction
<b>PSAX</b>	Parasternal short axis
<b>QPCR</b>	Quantitative polymerase chain reaction
<b>rhIL11</b>	Recombinant human interleukin 11
<b>RIPA</b>	Radioimmunoprecipitation assay buffer
<b>rmIL6</b>	Recombinant mouse interleukin 6
<b>rmIL11</b>	Recombinant mouse interleukin 11
<b>SEM</b>	Standard error of the mean
<b>STAT</b>	Signal transducer and activator of transcription
<b>TNF<math>\alpha</math></b>	Tumour necrosis factor-alpha
<b>UMAP</b>	Uniform Manifold Approximation and Projection
<b>vCMKO</b>	Viral mediated cardiomyocyte <i>Il11ra1</i> knockout
<b>VTI</b>	Velocity time integral
<b>WT</b>	Wild type

## Introduction

Interleukin 11 (IL11) is an elusive member of the interleukin 6 (IL6) family of cytokines, which collectively signal via the gp130 co-receptor. Following its identification in 1990<sup>1</sup> recombinant human IL11 (rhIL11) was found to increase megakaryocyte activity and peripheral platelet counts in mice<sup>2</sup>. Soon after, IL11 was developed as a therapeutic (Oprelvekin; Neumega) to increase platelet counts in patients with chemotherapy-induced thrombocytopenia, received FDA approval for this indication in 1998 and is still used to this day<sup>3,4</sup>. In recent years, longer-acting formulations of rhIL11 have been tested in pre-clinical studies and new clinical trials of PEGylated rhIL11 in patients are anticipated<sup>5</sup>.

RhIL11 was also trialled to increase platelet counts in patients with von Willebrand factor deficiency, myelodysplastic syndrome, cirrhosis and sepsis, and tested as a putative cytoprotective agent in numerous other conditions, including myocardial infarction<sup>6</sup> [**Table 1 and Suppl Table 1**]. However, it became apparent that IL11 is not required for basal or compensatory blood cell or platelet counts in mice or humans: IL11 is in fact redundant for haematopoiesis<sup>7,8</sup>. Thus, the effects of injection of high dose rhIL11 on platelets appear non-physiological and possibly reflect non-specific gp130 activity<sup>9,10</sup>.

Unfortunately, injection of rhIL11 into patients has severe and hitherto unexplained cardiac side effects. Up to 20% of patients given rhIL11 (50 mcg/kg) develop atrial arrhythmias, a high proportion of individuals develop heart failure and rare cases of ventricular arrhythmias and sudden death are reported<sup>11,12</sup>. Furthermore, serum natriuretic peptide levels become acutely and transiently elevated in patients receiving IL11 therapy, with B-natriuretic peptide levels sometimes exceeding those diagnostic of heart failure.

100 While IL11 was previously thought to be cytoprotective, anti-inflammatory and anti-fibrotic in  
 101 the heart<sup>13–15</sup> and other organs, recent studies by ourselves and others have challenged this  
 102 premise<sup>16–18</sup>. Indeed, experiments over the last five years have questioned the earlier literature  
 103 and IL11 is increasingly viewed as pro-inflammatory and pro-fibrotic. Given this large shift in  
 104 our understanding of IL11 and the fact that cardiomyocytes (CMs) robustly express IL11RA,  
 105 we devised experiments to determine whether IL11 is toxic to CMs and if this could explain  
 106 cardiac side effects associated with IL11 therapy in patients.

NCT Number	Title	Start Date	n	Status	Phase
<b>Thrombocytopenia</b>					
NCT03823079	Comparison of Interleukin-11 and rhTPO for Recurrent Colorectal Cancer Patients With Thrombocytopenia	Feb-19	50	Unknown status	2
NCT01663441	A Phase IIIa Study of Genetically Modified Recombinant Human Interleukin-11	Mar-15	62	Completed	3
NCT02314273	Effect of rhIL-11 in Patients With Thrombocytopenia for Childhood Acute Lymphocytic Leukaemia	Sep-11	120	Completed	4
NCT00886743	Study Evaluating The Effects Of Oprelvekin On Cardiac Repolarization In Subjects With Chemotherapy Induced Thrombocytopenia	Sep-09	19	Terminated	2
NCT00493181	Interleukin 11, Thrombocytopenia, Imatinib in Chronic Myelogenous Leukemia patients	Oct-05	8	Completed	2
<b>Coagulopathy</b>					
NCT00994929	Efficacy and Safety of IL-11 in DDAVP Unresponsive	Jan-10	9	Completed	2
NCT00524225	IL-11 in Adults With Von Willebrand Disease Undergoing Surgery	Feb-08	3	Terminated	2
NCT00524342	IL-11 in Women With Von Willebrand Disease and Refractory Menorrhagia	Jan-08	7	Completed	2
NCT00151125	Phase II Study of IL-11 (Neumega) in Von Willebrand Disease	Jul-04	12	Completed	2
<b>Inflammatory Bowel Disease</b>					
NCT00038922	Study Evaluating rhIL-11 in Left-Sided Ulcerative Colitis	Jun-02		Terminated	1
NCT00040521	Study Evaluating rhIL-11 in Active Crohn's Disease	Apr-02		Completed	2
<b>Other</b>					
NCT00012298	Radiolabeled Monoclonal Antibody Plus Rituximab With and Without Filgrastim and Interleukin-11 in Treating Patients With Relapsed or Refractory Non-Hodgkin's Lymphoma	Apr-01	81	Terminated	1/2
NCT03720340	Interleukin-11 Can Prevent and Treat of Radioactive Oral Mucitis	Oct-18	300	Unknown status	3

107 **Table 1. Human clinical trials registered with clinicaltrials.gov using recombinant human**  
108 **interleukin 11.**



# Methods

Detailed information on experimental methods of RNA and DNA analysis and cardiomyocyte isolation protocols are provided in the supplementary material.

## Animal studies

All mouse studies were conducted according to the Animals (Scientific Procedures) Act 1986 Amendment Regulations 2012 and approved by the Animal Welfare Ethical Review Body at Imperial College London. Animal experiments were carried out under UK Home Office Project License P108022D1 (September 2019). Wild type (WT) mice on a C57BL/6J background were purchased from Charles River (Cat#632). They were bred in a dedicated breeding facility and housed in a single room of the experimental animal facility with a 12-hour light-dark cycle and provided food and water *ad libitum*. The *Il11ra1* floxed mouse (C57BL/6-*Il11ra1*<sup>em1Cook/J</sup>, Jax:034465) has exons 4-7 of the *Il11ra1* gene flanked by loxP sites as has been described previously<sup>19</sup>. In the presence of Cre-recombinase excision of exon 4-7 results in a non-functional IL11 receptor.

Male myosin heavy chain 6 Cre (*Myh6*-Cre) mice (B6.FVB-Tg(*Myh6*-cre)2182Mds/J, Jax:011038) were purchased from Jax (Bar Harbor, Maine, United States) as heterozygotes. These mice were crossed with homozygous *Il11ra1* floxed females. In the second generation, mice from generation one, heterozygous for the *Il11ra1* flox allele and heterozygous for the Cre, were crossed with *Il11ra1* flox homozygotes to produce littermate experimental and control animals.

Recombinant mouse interleukin-11 (rmIL11) (Z03052, Genscript, Oxford, UK) was dissolved in phosphate-buffered saline (PBS) (14190144, ThermoFisher, MA, USA), and injected intraperitoneally (IP) at a dose of 200 mcg/kg unless otherwise stated. Control mice received

an equivalent volume of saline (2  $\mu$ L/kg). Recombinant mouse interleukin-6 (Z02767, Genscript) was dissolved in PBS and injected IP at a dose of 200 mcg/kg. Mice were randomly assigned to a treatment group using a random number generator and syringes for injection were prepared and blinded by a different investigator than administered the IP injection.

## Genotyping

Genotype was confirmed with ear-notch DNA samples. DNA was extracted using a sodium hydroxide digestion buffer, then neutralised with 1M Tris-HCl pH 8. *Il11ra1* flox genotype was confirmed with a single polymerase chain reaction (PCR) reaction yielding a PCR product at 163bp for the wild type allele or 197bp in the transgenic allele. *Myh6*-Cre mice were genotyped using two reactions for either the transgenic gene product of 295bp (or wild type gene product of 300bp) along with an internal positive control (200bp). Primers used in these reactions are detailed in supplementary table 2.

## Viral Vector

The viral vector used in this study, AAV9-cTNT-EGFP-T2A-iCre-WPRE (VB5413), was purchased from Vector Biolabs (Malvern, PA, USA). A codon optimised Cre was delivered using an AAV9 capsid and under the control of the *Tnnt2* promoter. This was linked to an enhanced green fluorescent protein (EGFP) reporter with a 2a self-cleaving linker.  $1 \times 10^{12}$  genome copies or an equivalent volume of saline were injected into the tail veins of 8 - 9 week old homozygous male *Il11ra1* flox mice and from this point mice were housed separately from saline-injected controls for 3 weeks prior to further experiments.

## Echocardiography

Echocardiography was performed under light isoflurane anaesthesia using a Vevo3100 imaging system and MX550D linear transducer (Fujifilm Visualsonic Inc, ON, Canada).

Anaesthesia was induced with 4% isoflurane for 1 minute and maintained with 1-2% isoflurane. Mice were allowed to equilibrate to the anaesthetic after induction for 9 minutes before imaging was started. Heart rate measurement from single lead electrocardiogram (ECG) recordings were taken at the completion of the equilibration period. Measurements of ventricular ejection fraction (LVEF) was measured from m-mode images taken in the parasternal short axis (PSAX) view at midventricular level and averaged across 3 heartbeats. Global circumferential strain (GCS) measurements were also taken from the PSAX view and analysed in a semi-automated fashion by the VevoStrain imaging software (VevoLab, version 5.5.0, Fujifilm Visualsonic). Aortic velocity time integral (VTI) was measured using pulse wave doppler in the aortic arch and an average taken from 3 heart beats. The investigator was blinded to the treatment group for all studies at both the imaging acquisition and analysis stages.

## qPCR

The tissue was washed in ice-cold PBS and snap-frozen in liquid nitrogen. Total RNA was extracted using TRIzol (15596026, Invitrogen, MA, USA,) in RNeasy columns (74106, Qiagen, MD, USA). cDNA was synthesised using Superscript Vilo Mastermix (11755050, Invitrogen). Gene expression analysis was performed using quantitative polymerase chain reaction (qPCR) with TaqMan gene expression assay in duplicate over 40 cycles. *Ill1ral*: custom TaqMan assay [**Suppl Table 3**], *Nppb*: Mm01255770\_g1, *Rrad*: Mm00451053\_m1. Gene expression data were normalised to *Gapdh* expression (Mm99999915\_g1) expression and fold change compared to control samples was calculated using  $2^{-\Delta\Delta Ct}$  method.

## RNASeq

8 week old male C57BL/6J mice were injected with rmIL11 (200 mcg/kg) or an equivalent volume of saline (2  $\mu$ L/kg). The left ventricle was excised and flash frozen 1, 3 or 6 hours after

injection. Libraries were sequenced on a NextSeq 2000 to generate a minimum of 20 million paired end 60bp reads per sample.

Raw RNAseq data and gene-level counts have been uploaded onto the NCBI Gene Expression Omnibus database and will be made available with accession number (GSE240804).

## Single nuclei RNAseq

Single nuclei sequencing was performed on flash frozen LV tissue that was extracted from 8 week old male C57BL/6J mice 3 hours after injection with rmIL11 (200mcg/kg) or saline (2μL/kg). The tissue was processed according to standard protocols as previously described<sup>20,21</sup>. Nuclei were purified by fluorescent activated cell sorting and libraries were sequenced using HiSeq 4000 (Illumina, CA, USA) with a minimum depth of 20,000–30,000 read pairs per nucleus.

All single nuclei sequence data generated and analyzed in this study have been deposited as BAM files at the NCBI Gene Expression Omnibus database and will be made available upon request.

## ATAC Seq

8 week old male C57BL/6J mice were given an IP injection with rmIL11 (200mcg/kg) or saline. The heart was excised 3 hours after injection and flash-frozen tissue was sent to Active Motif to perform assay for transposase-accessible chromatin with sequencing (ATAC-seq) analysis.

## Protein Analysis

Protein extraction was performed on flash frozen tissue using ice-cold Pierce RIPA buffer (89901, ThermoFisher) supplemented with protease inhibitors (11697498001, Roche, Basel, Switzerland) and phosphatase inhibitors (4906845001, Roche). Tissue was lysed using a

Qiagen Tissue Lyser II with metallic beads for 3 mins at 30Hz. Protein quantification was performed using a Pierce bicinchoninic acid assay colorimetric protein assay kit (23225, ThermoFisher). 10-20µg of protein was loaded per well and run on a 4-12% bis-tris precast sodium-dodecyl sulfate page gel (NP0323BOX, Invitrogen). Semi-dry transfer was performed using the TransBlot Turbo transfer system (1704150, BioRad, CA, USA) and the membrane was blocked in 5% bovine serum albumin (A3803, Sigma-Aldrich, MO, USA). Primary antibodies raised against the following targets were used: signal transducer and activator of transcription 3 (STAT3) (4904S, Cell signalling technology (CST), MA, USA), pSTAT3 Tyr705 (9145L, CST), Extracellular signal regulated kinase (ERK) (9101S, CST), pERK (4695S, CST), total c-Jun-N-terminal kinase (JNK) (sc-7345, Santa-Cruz, TX, USA), phospho-JNK (sc-6254, Santa-Cruz), green fluorescent protein (ab290, Abcam) Glyceraldehyde-3-phosphate dehydrogenase (GAPDH) (2118L, CST). Appropriate secondary horseradish peroxidase linked antibody was incubated for 1 hour with gentle agitation at room temperature and developed using chemiluminescence blotting substrate (1705061, BioRad or 34095, Thermofisher, depending on strength of signal).

## Cardiomyocyte extraction

CMs were extracted from the heart of 12 week old male C57BL/6J mice. Mice were deeply anaesthetized with ketamine and xylazine before the heart was harvested. Cells were incubated in Tyrode solution (1mM Ca, 1mM Mg) or Tyrode solution supplemented with rmIL11 (10 ng/mL) for 2 hours before recording. Cells were paced at 1Hz (10V, 10ms pulse width). Cell recordings were made using the Cytocypher high-throughput microscope (Cytocypher BV, Netherlands) and the automated cell finding system was used to identify and take recordings from 20 individual cells per heart per experimental condition. Calcium recordings were

performed by incubating CMs with Fura 2AM dye (1uM) for 20 mins before fluorescent recordings were taken.

## Statistics

Statistical analyses were performed in GraphPad Prism V9.5.0 unless otherwise stated. Normality testing was performed using the Shapiro-Wilk test. Hypothesis testing for single comparisons was done using an unpaired two ways Student's t-test for normally distributed data or by Mann-Whitney U test for non-normally distributed data.

Comparisons involving male and female mice were performed using a two-way analysis of variance (ANOVA) with Sidak's multiple comparisons testing. Changes in expression over multiple time points were analysed using a one-way ANOVA with Sidak's multiple comparisons testing. All graphs display the mean and standard error of the mean unless stated otherwise. P-values in RNA seq analysis were corrected for multiple testing using the false discovery rate (FDR) approach. A p-value and FDR of <0.05 was considered significant.

## Hierarchical testing of nested data

Statistical analysis of the data from high throughput microscopy of extracted cardiomyocyte experiments were analysed using a hierarchical statistical approach<sup>22</sup>. This approach tests for clustering within the data as may occur due to differences in the quality of myocyte preparation on different days. This uses a two-level random intercept model of linear regression. The analysis was performed using R-studio and the data was presented as the mean and standard deviation and effective n number taking the intraclass clustering into account.

## 243    Figures

244    Graphs were prepared in GraphPad Prism V9.5.0 and R studio (Version 2023.03.0).

245    Illustrations were created with Biorender.com and figures were arranged in Adobe Illustrator

246    (Version 23.0.4.).

## Results

### Injection of rmIL11 to mice causes acute left ventricular dysfunction

Injection of rmIL11 to male C57BL/6J mice resulted in a tachycardic response ( $544 \pm 13$  beats per minute (bpm),  $n=5$ ) as compared to mice injected with saline ( $433 \pm 12$  bpm,  $n=5$ ) (Mann Whitney test,  $p=0.0079$ ) [Fig1A, B]. Mice injected with rmIL11 injection had impaired LVEF ( $60.4\% \pm 3.1$  vs  $31.6 \pm 2.0$ ,  $p<0.0001$ ,  $n=5$  vs  $5$ ), reduced GCS ( $-30.8\% \pm 2.3$  vs  $-10.6 \pm 0.59$ ,  $p<0.0001$ ,  $n=5$  vs  $5$ ) and reduced VTI in the aortic arch ( $36.8\text{mm} \pm 1.9$  vs  $20.2 \pm 2.2$ ,  $p<0.0004$ ,  $n=5$  vs  $5$ ) compared to mice injected with saline [Fig1C-F]. To serve as a related cytokine control an equivalent dose (200 mcg/kg) of rmIL6 was injected which had no detectable acute effects on cardiac function [Fig1A-F & Suppl Fig S1A, B].

Dosing studies revealed that the effects of rmIL11 on heart rate and left ventricular (LV) function were dose-dependent, consistent with physiological binding to and activation of the IL11RA1 receptor. Cardiac impairment was evident at low doses and near-maximal effects were seen with a dose of 50 mcg/kg, which is the dose typically given daily to patients with thrombocytopenia post-chemotherapy [Fig1G]. The effect of rmIL11 was rapid with a nadir in cardiac function at 2 hours post injection and recovery seen by 6 hours. However, recovery in cardiac function was incomplete and mild LV impairment persisted for up to 7 days following a single dose of rmIL11 [Fig1H].

### IL11 causes impaired cardiomyocyte calcium handling

We next examined IL11 signalling pathways in cardiac extracts following rmIL11 injection, which revealed early and short-lived phosphorylation of signal transducer and activator of transcription 3 (p-STAT3) but no apparent ERK activation, which differs from acute signalling effects in the liver and other organs<sup>23</sup> [Fig1I & Suppl Fig S1C]. Phosphorylation of JNK is a



270 stress related signalling pathway shown to be elevated in the mouse liver following IL11  
 271 treatment<sup>23</sup>. In the myocardium JNK was phosphorylated at the 3 hour time point post rmIL11  
 272 injection by which stage STAT3 phosphorylation was declining [**Fig1I** & **& Suppl Fig S1D**].

273 The effect of IL11 directly on CMs was analysed *in vitro* by treating isolated adult mouse CMs  
 274 with rmIL11 for 2 hours. CMs treated with rmIL11 demonstrated impaired contractility, as  
 275 compared to control cells (Control:  $1.00 \pm 0.177$ ; rmIL11 (10 ng/mL):  $0.669 \pm 0.150$ ,  
 276  $p < 0.000266$ ) [**Fig1J**]. Intracellular calcium transients revealed blunting of the peak calcium  
 277 concentration during systole in the presence of rmIL11 (Control:  $1.00 \pm 0.0972$ ; rmIL11:  
 278  $0.781 \pm 0.0858$ ,  $p < 0.00019$ ) [**Fig1K**].

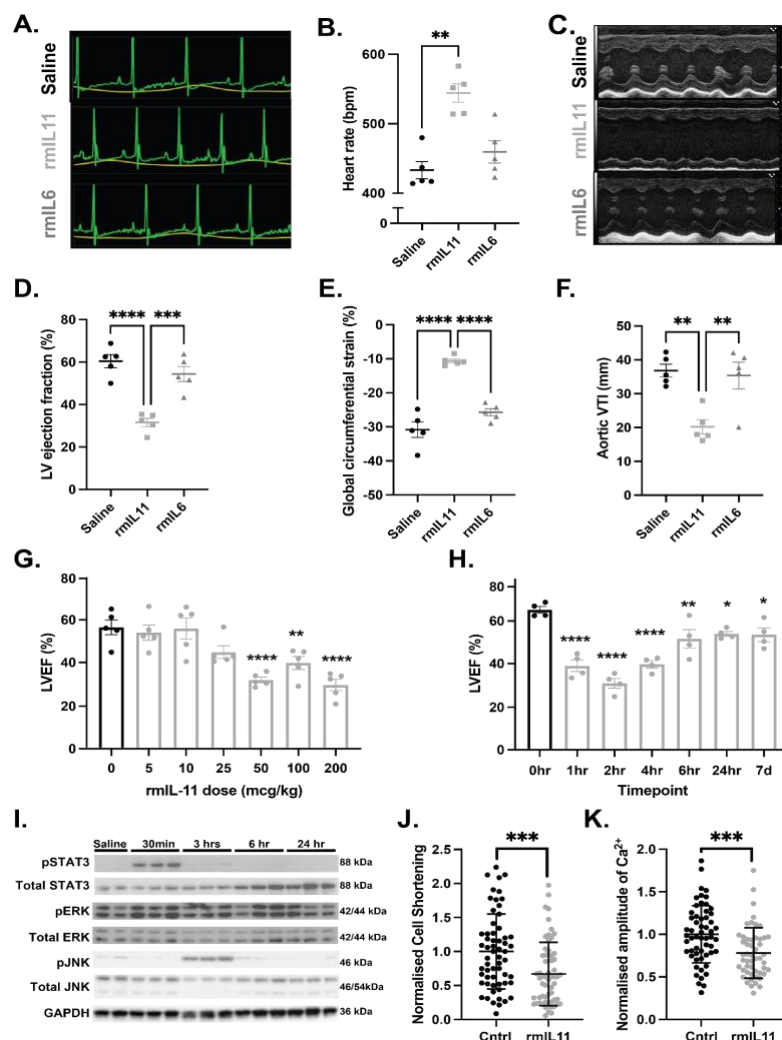


**Figure 1. IL11 causes acute heart failure and impairs cardiomyocyte calcium handling.**

Male C57BL/6J mice were injected with rmIL11 (200 mcg/kg) (■), rmIL6 (200 mcg/kg) (▲) or an equivalent volume of saline (2 µl/kg) (●). (A) Representative electrocardiogram traces were recorded under light anaesthesia, 2 hours after intraperitoneal (IP) injection of saline, rmIL11 or rmIL6. (B) Quantification of heart rate (n=5 per group). (C) Representative m-mode images from echocardiography performed 2 hours after injection of saline, rmIL11 or rmIL6. (D) Quantification of left ventricular ejection fraction (LVEF), (E) global circumferential strain and (F) velocity time integral at the aortic arch (VTI) in each group (n=5 per group). (G) LVEF 2 hours after IP injection of rmIL11 to male mice at 0, 5, 10, 25, 50, 100 and 200 mcg/kg (n=5 per dose). (H) LVEF at baseline, 1, 2, 4, 6, and 24 hours, and 7 days after IP injection of rmIL11 (200 mcg/kg) (n=4 per timepoint). (I) Western blot of myocardial lysates from C57BL/6J male mice at baseline and 0.5, 3, 6 and 24 hours after IP rmIL11 injection (200 mcg/kg). Blots are probed for pSTAT3, total STAT3, pERK, total ERK, pJNK, total JNK and GAPDH. CMs isolated from male C57BL/6J mice were treated *in vitro* for 2 hours with media supplemented with rmIL11 (10 ng/mL) or non-supplemented media (Cntrl) (n=3 mice, 20 cells per mouse) and assessed for (J) contractility (effective n=9.7) and (K) the systolic change of intracellular calcium concentration (effective n=12). *Statistics: One-way ANOVA with Sidak's multiple comparisons test. CM data: two level hierarchical clustering. Significance denoted as \*p<0.05, \*\*p<0.01, \*\*\*p<0.001, \*\*\*\*p<0.0001.*

## 299 IL11 causes cardiac inflammation

300 The robust and early activation of STAT3 by IL11 led us to explore transcriptional changes  
301 which might occur acutely within the myocardium in response to IL11 injection. Bulk RNA  
302 sequencing was performed on LV tissue at 1, 3 and 6 hours following injection of rmIL11 and  
303 compared to controls injected with saline.

304 Extensive and significant transcription changes were apparent at all timepoints (**1hr**, Up:145,  
305 Down:27; **3hr**, Up:450, Down:303; **6hr**: Up: 268, Down:169; Log<sub>2</sub>FC+/-1, FDR<0.05). Genes  
306 differentially regulated included early upregulation of acute inflammatory genes (*Il6*, *Il1b* and  
307 *Il33*), chemotactic factors such as (*Ccl2* and *Cxcl1*) and CM stress markers (*Nppb*, *Cnn2*,  
308 *Ankrd1*) [**Fig2A, B**]. Kyoto Encyclopedia of Genes and Genomes (KEGG) analysis of the  
309 differentially expressed genes at the 1-hour time point revealed the TNF $\alpha$ , NF- $\kappa$ B and  
310 JAK/STAT signalling were among the most significantly enriched terms [**Fig2C & Suppl Fig**  
311 **S2A, C**]. A similar group of inflammatory terms were highlighted by Hallmark Gene Set  
312 Enrichment Analysis including TNF $\alpha$  signalling via NF $\kappa$ B, IL6 JAK/STAT and interferon-  
313 gamma signalling [**Fig2D & Suppl Fig S2B, D**]. These transcriptional changes show that IL11  
314 drives an acute proinflammatory response in the heart that is associated with an impaired  
315 systolic function.

316 On closer inspection, the L-type calcium channel inhibitor *Rrad* was identified as one of the  
317 most significantly upregulated genes at 1 hour (Fc:4.91, FDR:3.2e-8) and 3 hours (Fc:4.51,  
318 FDR:9.2e-9) post rmIL11 treatment [**Fig2A, B**]. The *Rrad* protein product RAD-GTPase is a  
319 well-characterised and potent inhibitor of calcium current through L-type calcium channels<sup>24,25</sup>  
320 and its acute upregulation may account for the changes in calcium transients seen in isolated  
321 CM preparations.

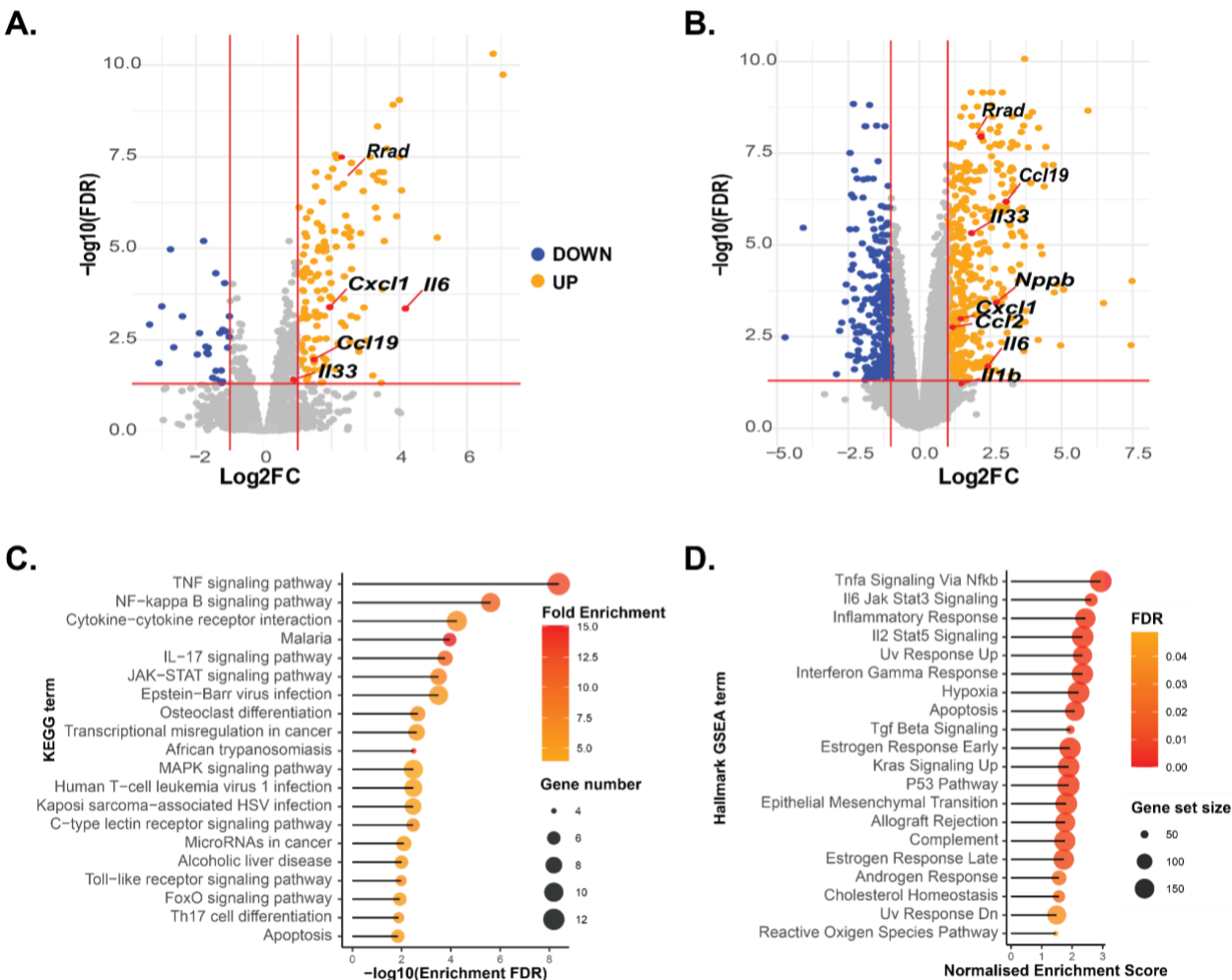


**Figure 2. Transcriptional changes in the myocardium following rmIL11 injection.** Volcano plot of all detected genes (A) 1 hour (n=3) and (B) 3 hours (n=4) after intraperitoneal injection of rmIL11 at 200 mcg/kg. Red lines are drawn at Log2Fc of 1 and -1 and FDR of 0.05. (C) Chart of most significantly enriched KEGG terms from at 1-hour post injection of rmIL11 ranked by FDR. (D) Gene set enrichment analysis of the most highly enriched Hallmark gene sets from RNAseq data at 1 hour after injection of rmIL11 ranked by normalised enrichment score.

## Single nuclear sequencing reveals a cardiomyocyte stress signature

To examine cell-specific transcriptional responses and define any potential changes in cell populations, we performed single nucleus RNA-sequencing (snRNAseq) experiments on hearts 3 hours post rmIL11 injection [Fig 3A, Suppl Fig S3A-C, S4A & Suppl Table 4]. This revealed no significant change in cell populations overall, excluding immune cell infiltration at this early time point [Fig 3B].

On closer analysis of CMs, this cell type segregated into four states with rmIL11-treated CM mostly localised to state 0 [Fig 3C, D]. This state is defined by the expression of cardiomyocyte stress factors including *Ankrd1*, *Ankrd23* and *Xirp2* [Figure 3E & Suppl Fig S4B]. *Ankrd1* and *Ankrd23* are stress-inducible ankyrin repeat proteins which are elevated in dilated cardiomyopathies<sup>26,27</sup>. *Xirp2* encodes cardiomyopathy-associated protein 3 and is upregulated in CMs in response to stress<sup>28,29</sup>. Expression of *Nppb*, a canonical heart failure gene, was similarly elevated [Fig 3E]. Overall, the most enriched pathway from KEGG analysis of CM-specific differentially expressed genes, irrespective of state, was “Ribosome” with 93 out of 130 genes significantly upregulated (Fold enrichment:4.5, FDR:2.3e-46), perhaps related to the large effects of IL11 on protein translation and/or a pro-hypertrophic response of stressed CMs [Suppl Fig S5]<sup>30</sup>.

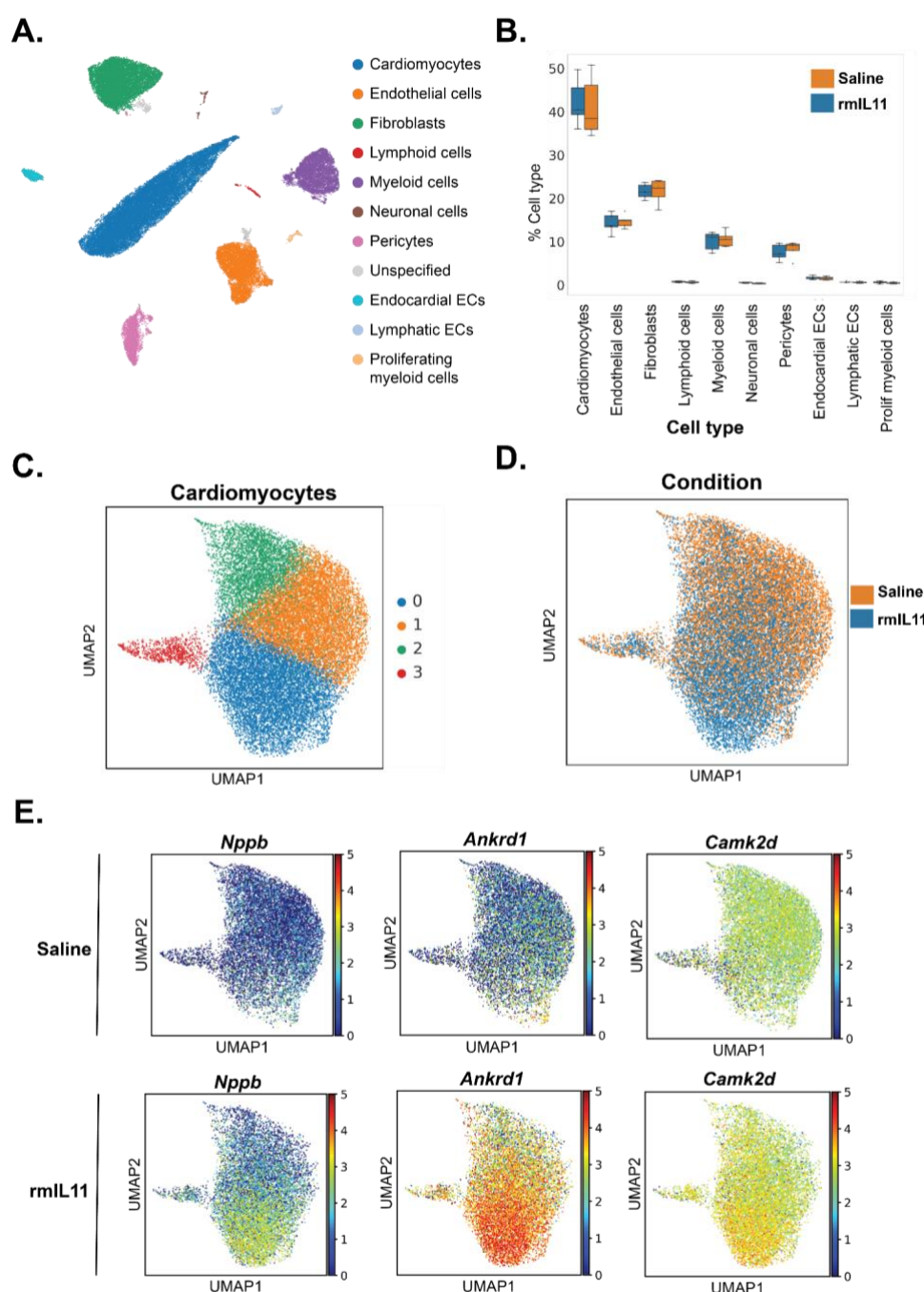


**Figure 3. Single nuclear RNA sequencing reveals an IL11-induced cardiomyocyte stress signature.** (A) UMAP embedding of all cell types from the left ventricle of male C57BL/6J mice 3 hours after intraperitoneal injection of rmIL11 (200 mcg/kg) or an equivalent volume of saline (n=5). (B) Comparison of cellular composition of the left ventricle in rmIL11 treated mice compared to saline treated mice. (C) UMAP embedding of cardiomyocyte fraction. 4 distinct clusters are identified based on gene expression. (D) UMAP embedding of cardiomyocytes annotated with the treatment group. (E) UMAP embedding of cardiomyocyte fraction of saline or rmIL11 treated cardiomyocytes annotated with relative expression of *Nppb*, *Ankrd1*, and *Camk2d*.

## ATAC-Seq highlights AP-1 family genes

To better understand the molecular changes induced by IL11 in the heart, we performed Assay for Transposase-Accessible Chromatin using sequencing (ATAC-seq) analysis. This methodology identifies regions of the genome undergoing epigenetic variation to make transcription factors binding sites more or less accessible.

Following IL11 administration, there were a large number of loci with variation in DNA accessibility (increased, 945; reduced, 445; shrunkenLog2FC:±0.3, Padj<0.1) [Fig 4A & Suppl Table 5]. The top twenty most differentially enriched regions [Fig 4B, C] include areas adjacent to *Camk2d*, *Ankrd1* and *Nppb*, stress and calcium handling genes that we had already found to be upregulated in CMs by snRNAseq [Fig 3E, Fig 4B & Suppl Table 4].

DNA motif analysis of sequences captured by ATAC-seq, revealed the most enriched motifs after rmIL11 treatment were targets for FOSL2 and JUNB transcription factors [Fig 4D & Suppl Table 6]. These genes belong to the activator protein-1 (AP-1) transcription factor family, which is important for cardiomyocyte stress responses, cardiac inflammation and fibrosis.<sup>31,32</sup> Notably, the STAT3 binding motif was also highly enriched.

We revisited our bulk RNA-seq data to examine the expression of the AP-1 transcription factor family transcripts after rmIL11 injection. This revealed that almost all of the AP-1 family transcripts are upregulated in the heart after rmIL11 [Fig 4E]. We then queried the snRNA-seq data and observed that *Fosl2*, *Junb*, *Atf6*, *Jun*, *Atf3* and *Mafg* are all significantly differentially expressed in cardiomyocytes following rmIL11 injection [Fig 4E and Suppl Table 4].



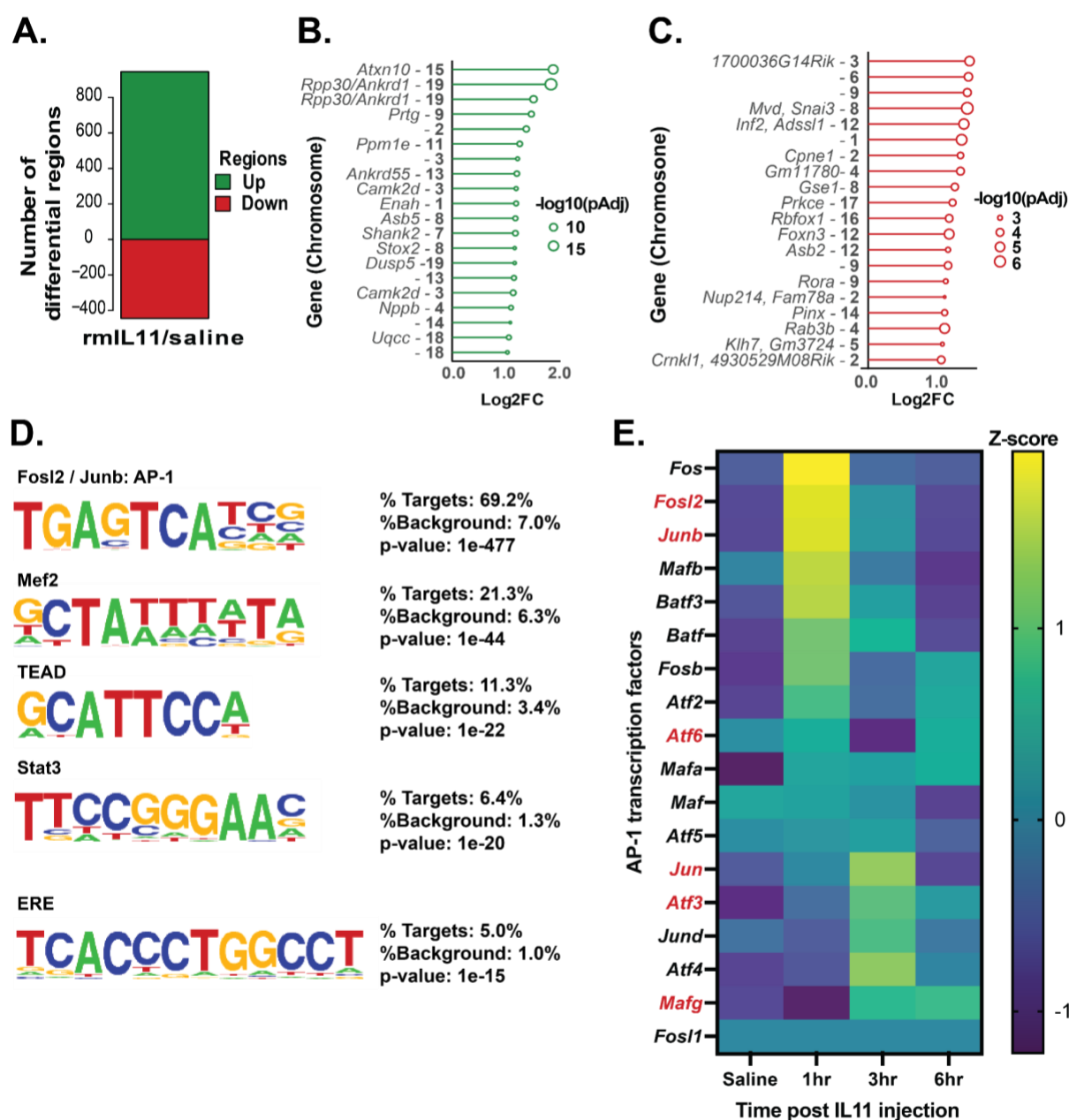


**Figure 4. ATAC-Seq reveals a stress signature that occurs acutely in the myocardium after rmIL11 injection.** (A) Number of positively and negatively enriched genomic regions identified by ATAC-Seq analysis of the myocardium 3 hours after injection of rmIL11 (n=4). (B) Top 20 most strongly enriched DNA regions in ATAC-seq analysis and adjacent genes, when present. (C) Top 20 most strongly negatively enriched DNA regions in ATAC-seq analysis and adjacent genes. (D) De novo Homer motif analysis of ATAC-seq data most highly enriched motifs in myocardial samples. (E) Heatmap of AP-1 transcription factor family members from bulk RNA sequencing data of myocardium at baseline, 1, 3 and 6 hours after rmIL11 injection. Genes differentially expressed in cardiomyocytes in single nuclear RNA sequencing data are highlighted in red.



## Viral-mediated CM-specific deletion of *Il11ral*

To test whether the acutely negative inotropic effects of IL11 and the signature of increased CM stress are specifically mediated via IL11 activity in CMs, we proceeded to conditionally delete *Il11ral* in CMs in the adult mouse. We used an adeno-associated virus serotype 9 (AAV9) vector to express *Tnnt2*-dependent *Cre*-recombinase in CMs of *Il11ral* floxed mice, which effectively removed the floxed exons to generate mice with viral-mediated deletion of *Il11ral* in CMs (vCMKO mice) [Fig 5A, B]. Effective transfection in the myocardium was confirmed by immunoblotting for GFP which is co-expressed with the *Cre*-recombinase [Fig 5C]. Notably, vCMKO mice had diminished myocardial p-STAT3 following injection of rmIL11, which demonstrates that IL11 activates JAK/STAT3 in CMs [Fig 5C, D].

As compared to mice injected with saline, WT mice injected with rmIL11 had impaired LVEF (WT+rmIL11: 26.5%±3.6), whereas vCMKO injected with rmIL11 had a mean LVEF (vCMKO+rmIL11: 50.8%±2.7) that was indistinguishable from saline-injected controls (vCMKO+saline: 57.0%±4.0) (n=3-5 per group) [Fig 5E]. Similar changes were seen in GCS (vCMKO+saline: -25.5%±1.9, vCMKO+rmIL11: -24.6%±1.4, WT+rmIL11: -11.1%±1.0, p<0.0001) and VTI in the aortic arch (vCMKO+saline: 37.8cm±1.9, vCMKO+rmIL11: 35.2cm±4.03, WT+rmIL11: 21.3cm±1.31, p<0.0371) [Fig 5F, G]. Interestingly, this experimental model still developed tachycardia following IL11 treatment, as seen in WT mice [Fig 5H].

We performed experiments in CMs isolated from adult mice. Unlike CMs isolated from WT animals [Fig 1J, K], CM from vCMKO mice did not have a reduction in cell shortening in response to stimulation with rmIL11, as compared to unstimulated cells (Cntrl: 1.0±0.11, vCMKO: 1.26±0.13, p=0.93, n=53.6). Similarly, peak calcium concentration was not blunted by rmIL11 in vCMKO CMs (Cntrl: 1.0±0.088, vCMKO: 0.83±0.076, p=0.15, n=36.3) [Fig 5I,

412 **J].** As such, IL11 effects in CMs are dependent on *Il1ral* expression in CMs. Consistent with  
 413 these changes in calcium signalling at a cellular level, qPCR of myocardial tissue of vCMKO  
 414 mice prevented elevation of *Rrad* compared to control mice following rmIL11 injection [**Fig**  
 415 **5K].**

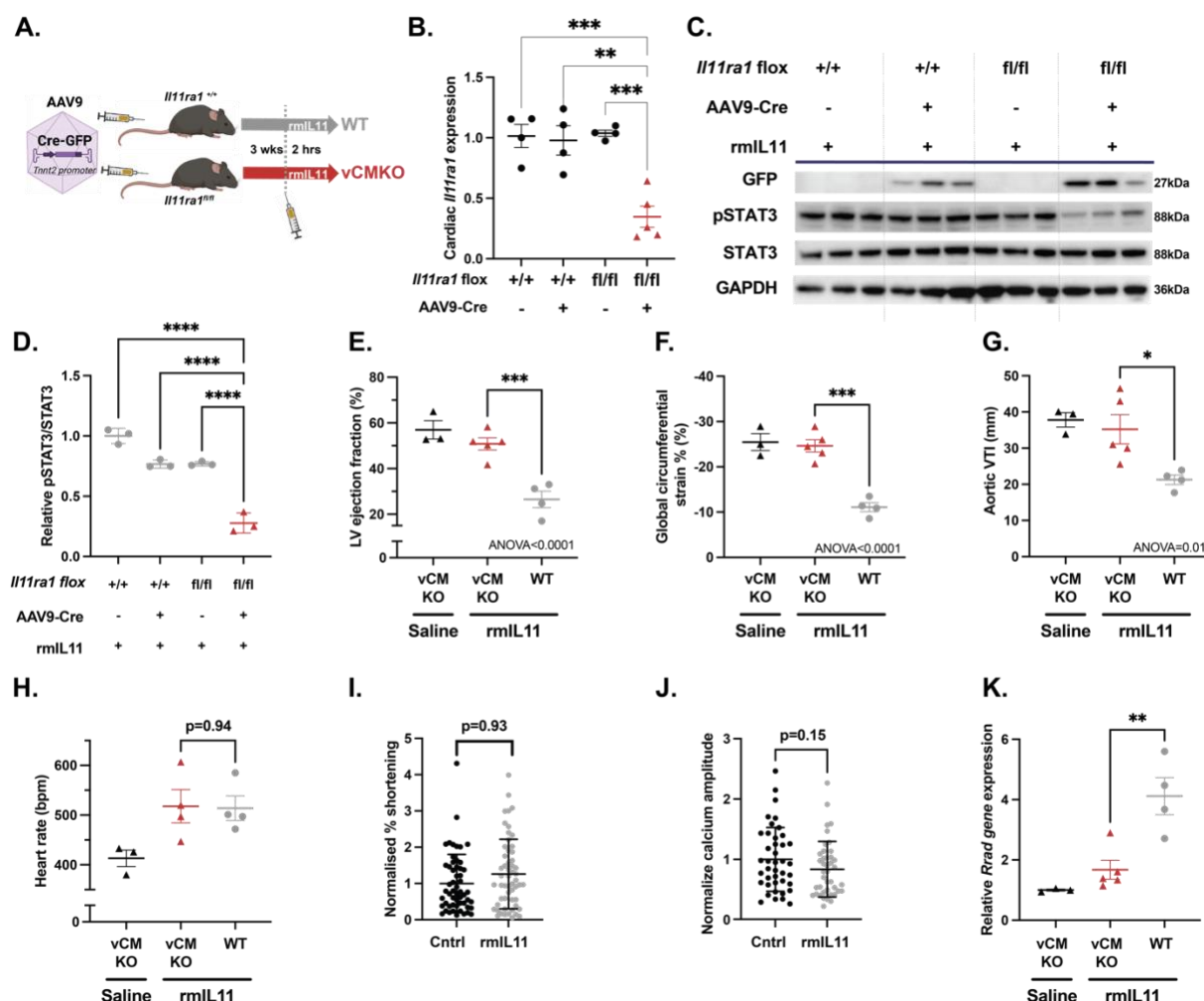


**Figure 5. Viral-mediated *Il11ra1* deletion in adult cardiomyocytes protects against IL11-driven cardiac dysfunction.** (A) Schematic of experimental design for AAV9 mediated delivery of *Tnnt2* promoter driven Cre-recombinase to male *Il11ra1<sup>fl/fl</sup>* or *Il11ra1<sup>+/+</sup>* mice. (B) QPCR of relative myocardial expression of *Il11ra1* in *Il11ra1<sup>+/+</sup>* or *Il11ra1<sup>fl/fl</sup>* injected with AAV9-Cre or vehicle. (C) Western blot from myocardial lysate following rmIL11 injection (200 mcg/kg) in *Il11ra1<sup>+/+</sup>* or *Il11ra1<sup>fl/fl</sup>* treated with either AAV9-Cre or saline (n=3). The membrane was probed with primary antibodies against GFP, pSTAT3, STAT3, and GAPDH. (D) Quantification of relative pSTAT3/STAT3 from (C). Echocardiographic assessment of vCMKO mice injected with rmIL11 (200 mcg/kg) (▲) or saline (▲) were compared to WT mice injected with rmIL11 (200 mcg/kg) (●). (E) Left ventricular ejection fraction, (F) global circumferential strain and (G) velocity time integral at the aortic arch and (H) heart rate were measured 2 hours after treatment (n=4). (I) Contractility (effective n = 53.6) and (J) peak calcium amplitude (effective n = 36.3) in CMs isolated from vCMKO mice and treated for 2 hours *in vitro* with rmIL11 containing media (10 ng/mL) or normal media (n=3 mice, 20 cells per mouse). (K) QPCR of myocardial expression of *Rrad* 2 hours vCMKO mice injected with rmIL11 (200 mcg/kg) (▲) or saline (▲) compared to WT mice injected with rmIL11 (200 mcg/kg) (●). Graphs CM data: mean ± standard deviation. Statistics: One-way ANOVA with Sidak's multiple comparisons testing. CM data: two level hierarchical clustering. Significance denoted as \**p*<0.05, \*\**p*<0.01, \*\*\**p*<0.001, \*\*\*\**p*<0.0001.

## Germline deletion of *Il11ra1* in cardiomyocytes

We then used a complementary, germline deletion methodology to validate the CM-specific effects of IL11 seen in vCMKO mice by crossing *Il11ra1* flox mice with *Myh6-Cre* (m6CMKO) mice<sup>33</sup> [Fig 6A]. This approach achieved a more pronounced and consistent knockdown of *Il11ra1* that enabled experiments to be scaled across sexes [Fig 6B]. As seen in the vCMKO strain, m6CMKO mice of both sexes had reduced p-STAT3 following rmIL11 injection, which further established effective *Il11ra1* locus recombination in this strain and reaffirms IL11-specific signalling in CMs [Fig 6C, D].

Having established the m6CMKO strain, we examined the effects of rmIL11 on cardiac function in these mice [Suppl Table 7]. When injected with rmIL11, *Il11ra1*<sup>fl/fl</sup> control mice had significantly reduced LVEFs whereas the LVEF of m6CMKO was similar to that of m6CMKO mice injected with saline [Fig 6E]. Similarly, following rmIL11 injection, GCS and VTI in the aortic arch were impaired in control mice expressing *Il11ra1* but not in m6CMKO mice [Fig 6F, G]. It was evident that the molecular and cardiovascular phenotypes of m6CMKO mice injected with rmIL11 largely replicated those observed in the vCMKO mice. However, different to the vCMKO strain, the m6CMKO mice were protected against IL11-induced tachycardia. [Fig 6H].

In molecular studies of myocardial extracts, *Nppb* was upregulated in *Il11ra1*<sup>fl/fl</sup> control mice in response to rmIL11 injection, but this was not seen in m6CMKO mice [Fig 6I]. Similarly, following rmIL11 injection the L-type calcium channel inhibitor *Rrad* was upregulated in *Il11ra1*<sup>fl/fl</sup> controls but not in m6CMKO mice [Fig 6J].

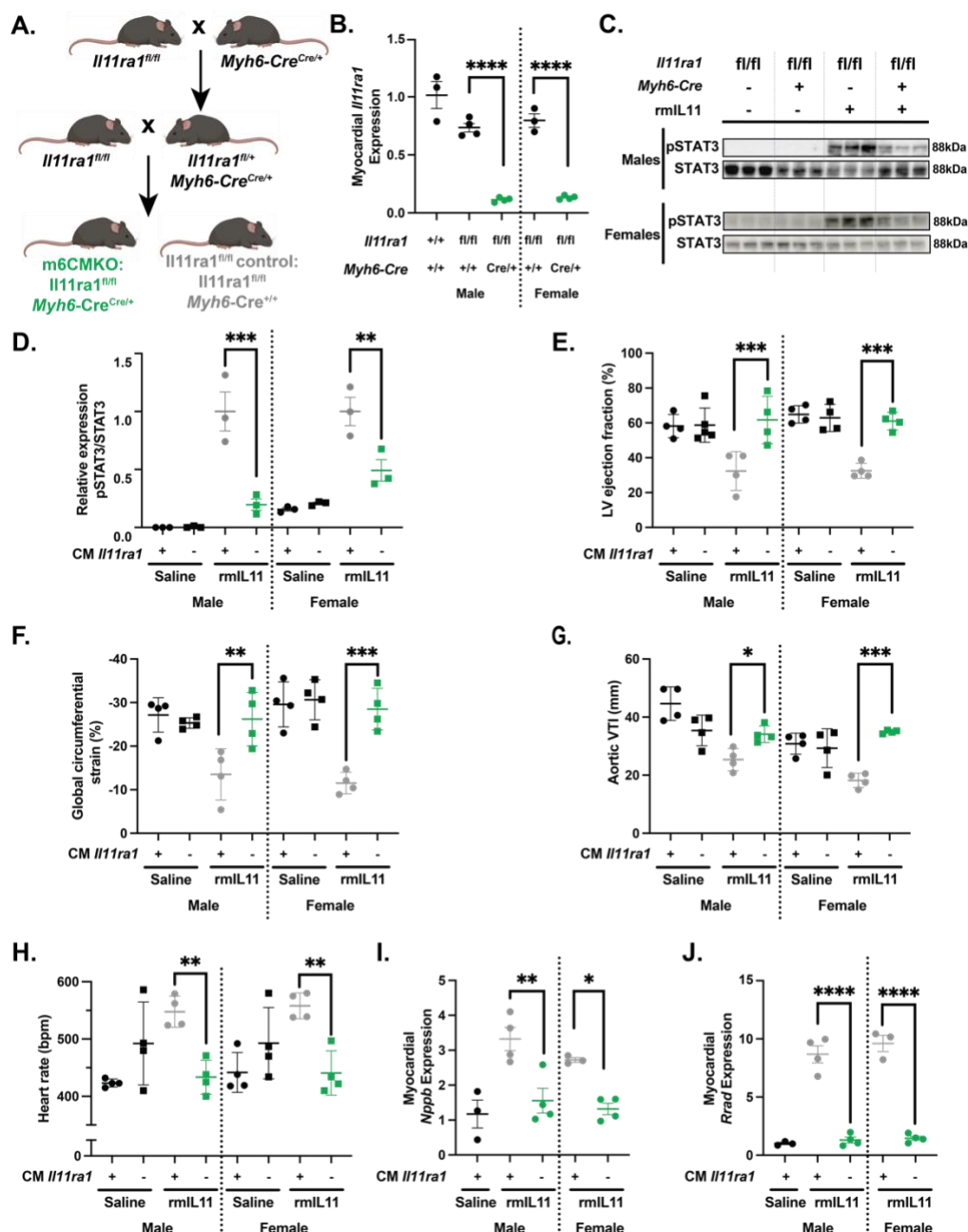


**Figure 6. Germline deletion of *Il11ra1* in cardiomyocytes prevents IL11-induced cardiac toxicities.** (A) Breeding strategy to generate m6CMKO mice and litter-mate *Il11ra1<sup>fl/fl</sup>* controls. (B) QPCR of *Il11ra1* gene expression in *Il11ra1<sup>fl/fl</sup>* controls and m6CMKO mice compared to male wild type C57BL/6J controls. (n=4) (C) Westerns blot of phospho-STAT3 and total STAT3 signalling in male and female *Il11ra1<sup>fl/fl</sup>* controls and m6CMKO mice with and without rmIL11 treatment. (D) Quantification of relative pSTAT and STAT3 expression. Male and female m6CMKO mice (CM *Il11ra1* -) were treated with saline (■) or rmIL11 (■) and compared to wild type mice (CM *Il11ra1* +) treated with saline (●) or rmIL11 (●) (n=4). (E) left ventricular ejection fraction, (F) global circumferential strain, (G) velocity time integral (VTI) in the aortic arch and (H) heart rate was measured 2 hours after rmIL11 injection. (n=4). QPCR analysis of relative expression of (I) *Nppb* and (J) *Rrad* in the myocardium following rmIL11 treatment of m6CMKO mice and *Il11ra1<sup>fl/fl</sup>* control mice (n=4). *Statistics:* Comparison between groups by two-way ANOVA with Sidak's multiple comparisons. *p*-values denoted as \**p*<0.05, \*\**p*<0.01, \*\*\**p*<0.001, \*\*\*\**p*<0.0001).

## JAK inhibition protects against IL11-induced cardiac dysfunction

Canonical IL11 signalling through the IL11RA/gp130/JAK/STAT3 pathway has recently been implicated in the acute pro-inflammatory effects of IL11<sup>34</sup> and activation of STAT3 in the heart was immediate and pronounced following IL11 injection [Fig 1I]. To determine the functional relevance of JAK/STAT3 activation in the heart we pretreated mice with ruxolitinib (30 mg/kg), which inhibits JAK1/2 activation, prior to injection of rmIL11 [Fig 7A].

We confirmed that administration of ruxolitinib at 30 mg/kg prevented activation of JAK/STAT3 signalling by immunoblotting [Fig 7B]. Having established the efficacy of ruxolitinib we studied its effect on cardiac physiology in 8 week old wild type male mice injected with rmIL11. Ruxolitinib alone had no effect on LV function [Fig 7C]. Following injection of rmIL11, and as compared to buffer injected controls, mice pretreated with ruxolitinib had better LVEF ( $60.5\% \pm 2.79$  vs  $35.2\% \pm 0.79$ ;  $p=0.0005$ ), GCS ( $-27.1\% \pm 1.56$  vs  $-13.6\% \pm 1.44$  vs,  $p=0.0009$ ) and aortic VTI ( $39.2\text{cm} \pm 10.9$  vs  $23.4\text{cm} \pm 1.92$ ,  $p=0.0001$ ) [Fig 7C-E]. Ruxolitinib pretreatment also prevented rmIL11-induced tachycardia ( $497 \pm 6.8$  vs  $419 \pm 14.1$ ,  $p=0.0008$ ) [Fig 7F]. As seen with m6CMKO, JAK inhibition prevented stress associated transcriptional changes in the heart of *Nppb* and *Rrad* [Fig 7G, H].

To exclude off-target effects and to replicate findings, the study was repeated with a second JAK inhibitor (tofacitinib, 20 mg/kg). As seen with ruxolitinib, pretreatment with tofacitinib protected against the varied deleterious effects of IL11 on cardiac function compared to vehicle treated controls: LVEF ( $59.0 \pm 4.16$ ,  $p=0.0007$ ), GCS ( $-25.7 \pm 2.10$ ,  $p=0.002$ ), VTI in the aortic arch ( $40.5 \pm 1.36$ ,  $p<0.0001$ ), and tachycardia ( $401 \pm 6.23$ ,  $p=0.0002$ ). [Fig 7C-E].

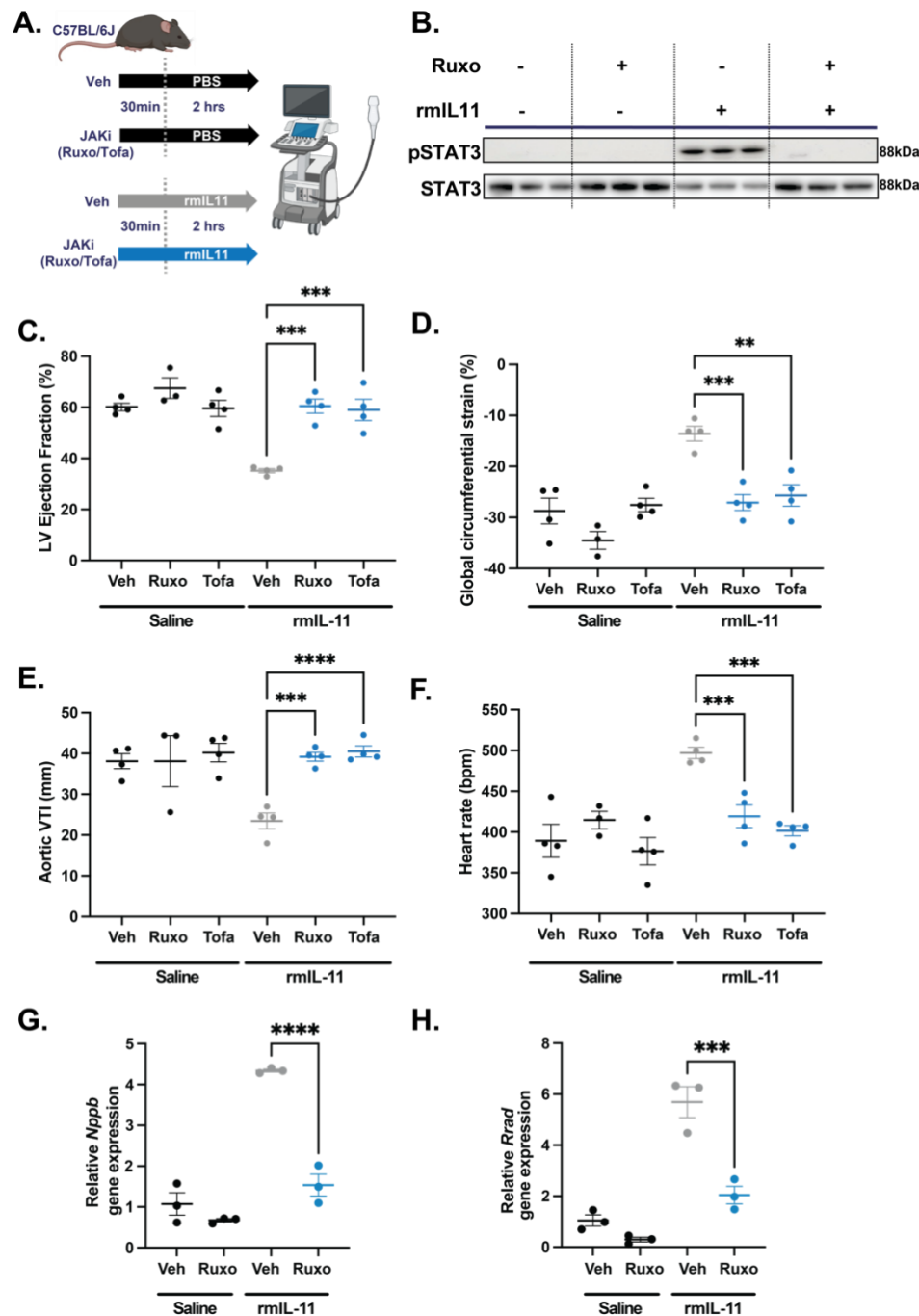


**Figure 7. The acute toxic effects of rmIL11 are mediated via JAK/STAT signalling.** (A) Schematic of the pretreatment of wild type male C57BL/6J mice with JAK inhibitor (JAKi) or vehicle (Veh) 30 mins before administration of recombinant mouse IL11 (rmIL11) or saline. (B) Western blot of myocardium lysate in mice treated with a combination of ruxolitinib (30 mg/kg) or vehicle and saline or rmIL11. Membranes have been probed for pSTAT3 and STAT3 (n=3). Mice treated with a combination of vehicle (Veh), ruxolitinib (Ruxo) or tofacitinib (Tofa) and either saline or rmIL11 had an echocardiogram performed 2 hours after treatment which measured (C) left ventricular ejection fraction, (D) global circumferential strain, (E) velocity time integral (VTI) in the aortic arch and (F) heart rate (n=4). QPCR of myocardial tissue from combinations of Ruxo and rmIL11 treatments of (G) *Nppb* expression and (H) *Rad* expression (n=3). Statistics: Comparison between groups by one-way ANOVA with Sidak's multiple comparisons test. Significance denoted as denoted \* $p < 0.05$ , \*\* $p < 0.01$ , \*\*\*\* $p < 0.0001$ .



## Discussion

In some healthcare systems, rhIL11 is used routinely to increase platelet counts in patients with thrombocytopenia but this can cause serious cardiac complications that are unexplained and thought non-specific. RhIL11 has also been trialled in a different context, as a cytoprotective agent, in patients across a range of other medical conditions (e.g. colitis, myocardial infarction, arthritis, cirrhosis), [Table 1 & Supl Table 1] as IL11 was previously thought to be anti-inflammatory and anti-fibrotic<sup>16</sup>. As such, many thousands of patients have received, and continue to receive, rhIL11 in clinical trials and as part of routine medical care. Long-acting formulations of rhIL11 have recently been devised and new clinical trials of rhIL11 are proposed<sup>5</sup>.

The cardiac side effects of rhIL11, while unexplained, have long been recognised and a small clinical trial was initiated in 2009 to determine if rhIL11 (50 mcg/kg) had an effect on cardiac conduction (NCT00886743). This trial was terminated prematurely at the request of the sponsor and no formal conclusions were made. Other studies looking at the effects of injection of human IL11 to adult rats showed no effects on cardiac phenotypes and studies of human atrial myocytes were similarly negative<sup>35,36</sup>. We suggest that, for these reasons, the severe cardiac side effects of rhIL11 therapy have been explained away as indirect, non-specific and thus sidelined<sup>36</sup>.

We found that injection of species-matched rmIL11 to mice caused acute and dose-dependent LV impairment that was mediated via IL11's action in IL11RA1 expressing CMs. CMs exposed to IL11 displayed perturbed calcium handling, upregulated cellular stress factors (*Ankrd1*, *Ankrd23*, *Xirp2*, *Nppb*) and had exhibited increased inflammation (TNF $\alpha$ , NF $\kappa$ B and JAK/STAT). These findings further redress the earlier literature on IL11 activity in the heart where it was believed to be anti-fibrotic<sup>14</sup>, which appears inaccurate<sup>30</sup>, and that it was



cytoprotective in CMs<sup>13–15</sup>, which we challenge here. In retrospect, the use of rhIL11 in a clinical trial of patients with myocardial infarction was likely ill-founded<sup>6</sup>.

The powerful enrichment of the AP-1 family of transcription factors following rmIL11 injection, seen in bulk RNA-seq, snRNA-seq and ATAC-seq was unexpected and likely has detrimental effects in the mouse heart<sup>31,37</sup>. AP-1 family activation is not immediately downstream of IL11:IL11RA:gp130 signalling and thus, the early IL11-stimulated activation of JAK/STAT3 likely primes CMs to upregulate, activate and respond to AP-1 transcription factors. In the injured zebrafish heart, AP-1 contributes to sarcomere disassembly and regeneration<sup>38</sup>, which is IL11-dependent<sup>39</sup>, providing an evolutionary context for IL11-mediated effects in the heart<sup>40</sup>.

Our use of two mouse models of CM-specific *Il11ra1* deletion show and replicate that the effects of rmIL11 on cardiac function are via direct cardiotoxic effects on CMs and are not explained by changes in circulating volume, as has previously been suggested<sup>36</sup>. The models used in this study involved the administration of a single dose of rmIL11 however in clinical practice, courses of therapy can involve daily infusions of rhIL11 for up to 21 days between chemotherapy cycles which are likely to compound the effect on the heart, specifically on fibrotic pathologies that are slow to establish<sup>30</sup>.

There are several limitations to our study. The discrepancy between the tachycardia seen in vCMKO but not m6CMKO mice suggests a direct effect of IL11 on sinoatrial node, which is differentially deleted for *Il11ra1* between the models, was not explored. We did not determine the putative roles of *Rrad* or *Camk2d* in IL11-induced contractile dysfunction, which should be investigated more fully in follow-on studies. Effects on human CMs were not examined, although we have observed conserved effects of IL11 on multiple cellular phenotypes in varied human and mouse cell types (e.g. fibroblasts, hepatocytes, epithelial cells)<sup>16,23</sup>. Whether

556 endogenous IL11 is toxic to CMs and negatively inotropic in heart failure syndromes is not  
 557 known and we cannot extrapolate from the data seen with acute, high dose injection of  
 558 recombinant protein. The cardiac side effects associated with IL11 include arrhythmias  
 559 (notably atrial fibrillation and flutter) that we did not study here.

560 In conclusion, we show for the first time that IL11 injection causes IL11RA-dependent, CM-  
 561 specific toxicities and acute heart failure. These data may explain the serious cardiac side  
 562 effects that occur with rhIL11 therapy, which have been overlooked. Our findings question the  
 563 ongoing use of rhIL11, and its further development<sup>5</sup>, in patients with thrombocytopenia while  
 564 identifying novel toxic effects of IL11 in the cardiomyocyte compartment of the heart.

## 565 Grant Funding:

566 This work was supported by grant funding from Wellcome Trust (203928/Z/16/Z), Foundation  
567 Leducq [16 CVD 03], the Medical Research Council (UK), The NIHR Biomedical Research  
568 Centre Imperial College London, the National Medical Research Council (NMRC) Singapore  
569 STaR award (NMRC/STaR/0011/2012) and a Goh Cardiovascular Research Award (Duke-  
570 NUS-GCR/2015/0014).

571 For the purpose of open access, the authors have applied a Creative Commons Attribution (CC  
572 BY) licence to any Author Accepted Manuscript version arising.

## 573 Disclosures

574 SAC is a co-inventor on a number of patent applications relating to the role of IL11 in human  
575 diseases that include the published patents: WO2017103108, WO2017103108 A2, WO  
576 2018/109174 A2, WO 2018/109170 A2. SAC is also a co-founder and shareholder of Enleofen  
577 Bio PTE LTD and VVB PTE LTD.

## 578 References

- 579 1. Paul SR, Bennett F, Calvetti JA, Kelleher K, Wood CR, O'Hara RM Jr, Leary AC,  
580 Sibley B, Clark SC, Williams DA, et al. Molecular cloning of a cDNA encoding  
581 interleukin 11, a stromal cell-derived lymphopoietic and hematopoietic cytokine. *Proc*  
582 *Natl Acad Sci U S A*. 1990;87:7512–7516.
- 583 2. Neben TY, Loebelenz J, Hayes L, McCarthy K, Stoudemire J, Schaub R, Goldman SJ.  
584 Recombinant human interleukin-11 stimulates megakaryocytopoiesis and increases  
585 peripheral platelets in normal and splenectomized mice. *Blood*. 1993;81:901–908.
- 586 3. Zhang J-J, Zhao R, Xia F, Li Y, Wang R-W, Guan X, Zhu J-G, Ma A-X. Cost-  
587 effectiveness analysis of rhTPO and rhIL-11 in the treatment of chemotherapy-induced  
588 thrombocytopenia in hematological tumors based on real-world data. *Ann Palliat Med*.  
589 2022;11:2709–2719.
- 590 4. Kaye JA. FDA licensure of NEUMEGA to prevent severe chemotherapy-induced  
591 thrombocytopenia. *Stem Cells*. 1998;16 Suppl 2:207–223.
- 592 5. Yu K-M, Lau JY-N, Fok M, Yeung Y-K, Fok S-P, Zhang S, Ye P, Zhang K, Li X, Li J,  
593 Xu Q, Wong W-T, Choo Q-L. Preclinical evaluation of the mono-PEGylated  
594 recombinant human interleukin-11 in cynomolgus monkeys. *Toxicol Appl Pharmacol*.  
595 2018;342:39–49.
- 596 6. Nakagawa M, Owada Y, Izumi Y, Nonin S, Sugioka K, Nakatani D, Iwata S, Mizutani  
597 K, Nishimura S, Ito A, Fujita S, Daimon T, Sawa Y, Asakura M, Maeda M, Fujio Y,  
598 Yoshiyama M. Four cases of investigational therapy with interleukin-11 against acute  
599 myocardial infarction. *Heart Vessels*. 2016;31:1574–1578.
- 600 7. Nandurkar HH, Robb L, Tarlinton D, Barnett L, Köntgen F, Begley CG. Adult mice  
601 with targeted mutation of the interleukin-11 receptor (IL11Ra) display normal  
602 hematopoiesis. *Blood*. 1997;90:2148–2159.
- 603 8. Ng B, Widjaja AA, Viswanathan S, Dong J, Chothani SP, Lim S, Shekeran SG, Tan J,  
604 McGregor NE, Walker EC, Sims NA, Schafer S, Cook SA. Similarities and differences  
605 between IL11 and IL11RA1 knockout mice for lung fibro-inflammation, fertility and  
606 craniosynostosis. *Sci Rep*. 2021;11:14088.
- 607 9. Tanaka M, Hirabayashi Y, Sekiguchi T, Inoue T, Katsuki M, Miyajima A. Targeted  
608 disruption of oncostatin M receptor results in altered hematopoiesis. *Blood*.  
609 2003;102:3154–3162.
- 610 10. Denton CP, Del Galdo F, Khanna D, Vonk MC, Chung L, Johnson SR, Varga J, Furst  
611 DE, Temple J, Zecchin C, Csomor E, Lee A, Wisniacki N, Flint SM, Reid J. Biological  
612 and clinical insights from a randomised phase II study of an anti-oncostatin M  
613 monoclonal antibody in systemic sclerosis. *Rheumatology* [Internet]. 2022;Available  
614 from: <http://dx.doi.org/10.1093/rheumatology/keac300>
- 615 11. Smith JW 2nd. Tolerability and side-effect profile of rhIL-11. *Oncology* . 2000;14:41–  
616 47.

12. Liu N-W, Huang X, Liu S, Liu W-J, Wang H, Wang W, Lu Y. Elevated BNP caused by recombinant human interleukin-11 treatment in patients with chemotherapy-induced thrombocytopenia. *Support Care Cancer* [Internet]. 2019; Available from: <http://dx.doi.org/10.1007/s00520-019-04734-z>
13. Obana M, Miyamoto K, Murasawa S, Iwakura T, Hayama A, Yamashita T, Shiragaki M, Kumagai S, Miyawaki A, Takewaki K, Matsumiya G, Maeda M, Yoshiyama M, Nakayama H, Fujio Y. Therapeutic administration of IL-11 exhibits the postconditioning effects against ischemia-reperfusion injury via STAT3 in the heart. *Am J Physiol Heart Circ Physiol*. 2012;303:H569-77.
14. Obana M, Maeda M, Takeda K, Hayama A, Mohri T, Yamashita T, Nakaoka Y, Komuro I, Takeda K, Matsumiya G, Azuma J, Fujio Y. Therapeutic activation of signal transducer and activator of transcription 3 by interleukin-11 ameliorates cardiac fibrosis after myocardial infarction. *Circulation*. 2010;121:684–691.
15. Kimura R, Maeda M, Arita A, Oshima Y, Obana M, Ito T, Yamamoto Y, Mohri T, Kishimoto T, Kawase I, Fujio Y, Azuma J. Identification of cardiac myocytes as the target of interleukin 11, a cardioprotective cytokine. *Cytokine*. 2007;38:107–115.
16. Cook SA, Schafer S. Hiding in Plain Sight: Interleukin-11 Emerges as a Master Regulator of Fibrosis, Tissue Integrity, and Stromal Inflammation. *Annu Rev Med*. 2020;71:263–276.
17. Corden B, Adami E, Sweeney M, Schafer S, Cook SA. IL-11 in cardiac and renal fibrosis: Late to the party but a central player. *Br J Pharmacol*. 2020;177:1695–1708.
18. Sweeney M, O'Fee K, Villanueva-Hayes C, Rahman E, Lee M, Vanezis K, Andrew I, Lim W-W, Widjaja A, Barton PJR, Cook SA. Cardiomyocyte-Restricted Expression of IL11 Causes Cardiac Fibrosis, Inflammation, and Dysfunction. *Int J Mol Sci*. 2023;24:12989.
19. Ng B, Dong J, Viswanathan S, Widjaja AA, Paleja BS, Adami E, Ko NSJ, Wang M, Lim S, Tan J, Chothani SP, Albani S, Schafer S, Cook SA. Fibroblast-specific IL11 signaling drives chronic inflammation in murine fibrotic lung disease. *FASEB J*. 2020;34:11802–11815.
20. Litviňuková M, Talavera-López C, Maatz H, Reichart D, Worth CL, Lindberg EL, Kanda M, Polanski K, Heinig M, Lee M, Nadelmann ER, Roberts K, Tuck L, Fasouli ES, DeLaughter DM, McDonough B, Wakimoto H, Gorham JM, Samari S, Mahbubani KT, Saeb-Parsy K, Patone G, Boyle JJ, Zhang H, Zhang H, Viveiros A, Oudit GY, Bayraktar OA, Seidman JG, Seidman CE, Nosedá M, Hubner N, Teichmann SA. Cells of the adult human heart. *Nature*. 2020;588:466–472.
21. Litvinukova M, Lindberg E, Maatz H, Zhang H, Radke M, Gotthardt M, Saeb-Parsy K, Teichmann S, Hübner N. Single cell and single nuclei analysis human heart tissue v1 [Internet]. 2018 [cited 2023 Aug 30]; Available from: <https://www.protocols.io/view/single-cell-and-single-nuclei-analysis-human-heart-x54v98pkml3e/v1>
22. Sikkil MB, Francis DP, Howard J, Gordon F, Rowlands C, Peters NS, Lyon AR,

- Harding SE, MacLeod KT. Hierarchical statistical techniques are necessary to draw reliable conclusions from analysis of isolated cardiomyocyte studies. *Cardiovasc Res*. 2017;113:1743–1752.
23. Widjaja AA, Dong J, Adami E, Viswanathan S, Ng B, Pakkiri LS, Chothani SP, Singh BK, Lim WW, Zhou J, Shekeran SG, Tan J, Lim SY, Goh J, Wang M, Holgate R, Hearn A, Felkin LE, Yen PM, Dear JW, Drum CL, Schafer S, Cook SA. Redefining IL11 as a regeneration-limiting hepatotoxin and therapeutic target in acetaminophen-induced liver injury. *Sci Transl Med* [Internet]. 2021;13. Available from: <http://dx.doi.org/10.1126/scitranslmed.aba8146>
24. Ahern BM, Levitan BM, Veeranki S, Shah M, Ali N, Sebastian A, Su W, Gong MC, Li J, Stelzer JE, Andres DA, Satin J. Myocardial-restricted ablation of the GTPase RAD results in a pro-adaptive heart response in mice. *J Biol Chem*. 2019;294:10913–10927.
25. Papa A, Zakharov SI, Katchman AN, Kushner JS, Chen B-X, Yang L, Liu G, Jimenez AS, Eisert RJ, Bradshaw GA, Dun W, Ali SR, Rodrigues A, Zhou K, Topkara V, Yang M, Morrow JP, Tsai EJ, Karlin A, Wan E, Kalocsay M, Pitt GS, Colecraft HM, Ben-Johny M, Marx SO. Rad regulation of CaV1.2 channels controls cardiac fight-or-flight response. *Nat Cardiovasc Res*. 2022;1:1022–1038.
26. Ling SSM, Chen Y-T, Wang J, Richards AM, Liew OW. Ankyrin Repeat Domain 1 Protein: A Functionally Pleiotropic Protein with Cardiac Biomarker Potential. *Int J Mol Sci* [Internet]. 2017;18. Available from: <http://dx.doi.org/10.3390/ijms18071362>
27. Zhang N, Ye F, Zhou Y, Zhu W, Xie C, Zheng H, Chen H, Chen J, Xie X. Cardiac ankyrin repeat protein contributes to dilated cardiomyopathy and heart failure. *FASEB J*. 2021;35:e21488.
28. McCalmon SA, Desjardins DM, Ahmad S, Davidoff KS, Snyder CM, Sato K, Ohashi K, Kielbasa OM, Mathew M, Ewen EP, Walsh K, Gavras H, Naya FJ. Modulation of angiotensin II-mediated cardiac remodeling by the MEF2A target gene Xirp2. *Circ Res*. 2010;106:952–960.
29. Dewenter M, Pan J, Knödler L, Tzschöckel N, Henrich J, Cordero J, Dobrev G, Lutz S, Backs J, Wieland T, Vettel C. Chronic isoprenaline/phenylephrine vs. exclusive isoprenaline stimulation in mice: critical contribution of alpha1-adrenoceptors to early cardiac stress responses. *Basic Res Cardiol*. 2022;117:15.
30. Schafer S, Viswanathan S, Widjaja AA, Lim W-W, Moreno-Moral A, DeLaughter DM, Ng B, Patone G, Chow K, Khin E, Tan J, Chothani SP, Ye L, Rackham OJL, Ko NSJ, Sahib NE, Pua CJ, Zhen NTG, Xie C, Wang M, Maatz H, Lim S, Saar K, Blachut S, Petretto E, Schmidt S, Putoczki T, Guimarães-Camboa N, Wakimoto H, van Heesch S, Sigmundsson K, Lim SL, Soon JL, Chao VTT, Chua YL, Tan TE, Evans SM, Loh YJ, Jamal MH, Ong KK, Chua KC, Ong B-H, Chakaramakkil MJ, Seidman JG, Seidman CE, Hubner N, Sin KYK, Cook SA. IL-11 is a crucial determinant of cardiovascular fibrosis. *Nature*. 2017;552:110–115.
31. Stellato M, Dewenter M, Rudnik M, Hukara A, Özsoy Ç, Renoux F, Pachera E, Gantenbein F, Seebeck P, Uhtjaerv S, Osto E, Razansky D, Klingel K, Henes J, Distler O, Błyszczuk P, Kania G. The AP-1 transcription factor Fos1-2 drives cardiac fibrosis



and arrhythmias under immunofibrotic conditions. *Commun Biol.* 2023;6:161.

32. van Duijvenboden K, de Bakker DEM, Man JCK, Janssen R, Günthel M, Hill MC, Hooijkaas IB, van der Made I, van der Kraak PH, Vink A, Creemers EE, Martin JF, Barnett P, Bakkers J, Christoffels VM. Conserved NPPB+ Border Zone Switches From MEF2- to AP-1-Driven Gene Program. *Circulation.* 2019;140:864–879.
33. Agah R, Frenkel PA, French BA, Michael LH, Overbeek PA, Schneider MD. Gene recombination in postmitotic cells. Targeted expression of Cre recombinase provokes cardiac-restricted, site-specific rearrangement in adult ventricular muscle in vivo. *J Clin Invest.* 1997;100:169–179.
34. Widjaja AA, Chothani S, Viswanathan S, Goh JWT, Lim W-W, Cook SA. IL11 Stimulates IL33 Expression and Proinflammatory Fibroblast Activation across Tissues. *Int J Mol Sci* [Internet]. 2022;23. Available from: <http://dx.doi.org/10.3390/ijms23168900>
35. Sartiani L, De Paoli P, Lonardo G, Pino R, Conti AA, Cerbai E, Pelleg A, Belardinelli L, Mugelli A. Does recombinant human interleukin-11 exert direct electrophysiologic effects on single human atrial myocytes? *J Cardiovasc Pharmacol.* 2002;39:425–434.
36. Xu J, Ren J-F, Mugelli A, Belardinelli L, Keith JC Jr, Pelleg A. Age-dependent atrial remodeling induced by recombinant human interleukin-11: implications for atrial flutter/fibrillation. *J Cardiovasc Pharmacol.* 2002;39:435–440.
37. Freire G, Ocampo C, Ilbawi N, Griffin AJ, Gupta M. Overt expression of AP-1 reduces alpha myosin heavy chain expression and contributes to heart failure from chronic volume overload. *J Mol Cell Cardiol.* 2007;43:465–478.
38. Beisaw A, Kuenne C, Guenther S, Dallmann J, Wu C-C, Bentsen M, Looso M, Stainier DYR. AP-1 Contributes to Chromatin Accessibility to Promote Sarcomere Disassembly and Cardiomyocyte Protrusion During Zebrafish Heart Regeneration. *Circ Res.* 2020;126:1760–1778.
39. Allanki S, Strilic B, Scheinberger L, Onderwater YL, Marks A, Günther S, Preussner J, Kikhi K, Looso M, Stainier DYR, Reischauer S. Interleukin-11 signaling promotes cellular reprogramming and limits fibrotic scarring during tissue regeneration. *Sci Adv.* 2021;7:eabg6497.
40. Cook SA. The Pathobiology of Interleukin 11 in Mammalian Disease is Likely Explained by its Essential Evolutionary Role for Fin Regeneration. *J Cardiovasc Transl Res* [Internet]. 2023;Available from: <http://dx.doi.org/10.1007/s12265-022-10351-9>
41. Dobin A, Davis CA, Schlesinger F, Drenkow J, Zaleski C, Jha S, Batut P, Chaisson M, Gingeras TR. STAR: ultrafast universal RNA-seq aligner. *Bioinformatics.* 2013;29:15–21.
42. Liao Y, Smyth GK, Shi W. featureCounts: an efficient general purpose program for assigning sequence reads to genomic features. *Bioinformatics.* 2014;30:923–930.

43. Robinson MD, McCarthy DJ, Smyth GK. edgeR: a Bioconductor package for differential expression analysis of digital gene expression data. *Bioinformatics*. 2010;26:139–140.
44. Mootha VK, Lindgren CM, Eriksson K-F, Subramanian A, Sihag S, Lehar J, Puigserver P, Carlsson E, Ridderstråle M, Laurila E, Houstis N, Daly MJ, Patterson N, Mesirov JP, Golub TR, Tamayo P, Spiegelman B, Lander ES, Hirschhorn JN, Altshuler D, Groop LC. PGC-1alpha-responsive genes involved in oxidative phosphorylation are coordinately downregulated in human diabetes. *Nat Genet*. 2003;34:267–273.
45. Subramanian A, Tamayo P, Mootha VK, Mukherjee S, Ebert BL, Gillette MA, Paulovich A, Pomeroy SL, Golub TR, Lander ES, Mesirov JP. Gene set enrichment analysis: a knowledge-based approach for interpreting genome-wide expression profiles. *Proc Natl Acad Sci U S A*. 2005;102:15545–15550.
46. Kanehisa M, Goto S. KEGG: kyoto encyclopedia of genes and genomes. *Nucleic Acids Res*. 2000;28:27–30.
47. Kanehisa M, Furumichi M, Sato Y, Kawashima M, Ishiguro-Watanabe M. KEGG for taxonomy-based analysis of pathways and genomes. *Nucleic Acids Res*. 2023;51:D587–D592.
48. Ge SX, Jung D, Yao R. ShinyGO: a graphical gene-set enrichment tool for animals and plants. *Bioinformatics*. 2020;36:2628–2629.
49. Buenrostro JD, Giresi PG, Zaba LC, Chang HY, Greenleaf WJ. Transposition of native chromatin for fast and sensitive epigenomic profiling of open chromatin, DNA-binding proteins and nucleosome position. *Nat Methods*. 2013;10:1213–1218.
50. Corces MR, Trevino AE, Hamilton EG, Greenside PG, Sinnott-Armstrong NA, Vesuna S, Satpathy AT, Rubin AJ, Montine KS, Wu B, Kathiria A, Cho SW, Mumbach MR, Carter AC, Kasowski M, Orloff LA, Risca VI, Kundaje A, Khavari PA, Montine TJ, Greenleaf WJ, Chang HY. An improved ATAC-seq protocol reduces background and enables interrogation of frozen tissues. *Nat Methods*. 2017;14:959–962.